Oceanographic Causes for Transarctic Ice Transport of River Discharge

I. Dmitrenko[1], P. Golovin[1], V. Gribanov[1] and H. Kassens[2]

(1) State Research Center - Arctic and Antarctic Research Institute, 38 Bering St., 199226 St. Petersburg, Russia

(2) GEOMAR Forschungszentrum für marine Geowissenschaften, Wischhofstrasse 1-3, D 24148 Kiel, Germany

Received 3 March 1997 and accepted in revised form 8 February 1998

Abstract - The influence of river discharge on ice-hydrological conditions was investigated during expeditions in the Laptev Sea in 1994, 1995 and 1996 during different seasons of the year within the framework of the Russian-German project "Laptev Sea System". A combined analysis of both ice satellite and CTD observations has shown that the formation and distribution of the fast ice edge is dependent on vertical heat exchange processes with the warm subsurface water layer underlying river water over a depth range of 10 to 25 m. It is formed during the summertime in areas affected by river discharge, which spreads as a result of warm surface water converging at the discharge fronts. Calculations show that advection of heat and double-diffusive convection are the most efficient modes of heat transport to the growing ice at the periphery of the freshened zone. Their values are sufficient to reduce the ice thickness at the periphery of the discharge zone by more than half. This leads to a fast ice edge much further south than the northern limit of the freshened zone. As a result, a considerable amount of riverine dissolved and suspended matter is incorporated into drifting ice and hence into transarctic ice transport.

Introduction

One of the main objectives of the Russian-German multidisciplinary research project the "Laptev Sea System" is to investigate the pathways and mechanisms of suspended matter and sediment transport from the Laptev Sea to the Arctic Ocean. The transarctic ice transport of sediments and suspended matter incorporated into sea ice at freezing was suggested (e.g. Eicken et al., 1997). Since the Lena River is one of the main sources of dissolved and suspended matter supply to the Laptev Sea, it is especially important to investigate the fate of river water.

Previous expedition studies have shown that the majority of suspended matter is distributed in accordance with the spreading of river water and that it is centered in the upper 7-9 m. In this case, it is expected that the most intense incorporation of suspended matter coincides with regions where river discharge was located at the onset of freezing (Dmitrenko et al., in press). Under the influence of river discharge, the upper sea layer is significantly diluted („freshened„). The resulting strong density stratification in most regions (except in shallow water) prevents penetration of sea water mixing processes down to the sea floor. This in turn inhibits the transport of bottom sediments to the sea surface. However, suspended matter concentrated in the surface freshened layer can be incorporated into the forming ice after the onset of freezing. This ice forms a massif of fast ice or drifting first-year ice located beyond the fast ice limits (including flaw polynyas). The latter is extremely important in terms of potential ice transport of sediments. Drift trajectories of GPS-buoys set up on fast ice north-east of the Lena delta in the spring of 1996 confirmed that fast ice can melt in place. However, first-year drifting ice can be entrained to the transarctic drift. Thus, one factor determining the transarctic sea ice transport of river discharge is the type of ice cover into which the river discharge is incorporated at freezing. Hence, this study focuses on the influence of river discharge on the extent of the fast ice cover.

In: Kassens, H., H.A. Bauch, I. Dmitrenko, H. Eicken, H.-W. Hubberten, M. Melles, J. Thiede and L. Timokhov (eds.) Land-Ocean Systems in the Siberian Arctic: Dynamics and History. Springer-Verlag, Berlin, 1999, 73-92.

Materials and methods

The analysis and calculations were based on CTD-soundings during the expeditions Transdrift II (September 1994), Transdrift III (October 1995) and during the winter portion of the Transdrift IV expedition (May 1996; see Figure 1). On the Transdrift II expedition, observations were made from aboard the R/V "Professor Multanovsky" in the ice-free region of the Laptev Sea. During the Transdrift III, expedition work was carried out aboard the icebreaker "Kapitan Dranitsyn" or from the ice cover at a distance of not more than 100 m from the icebreaker. The stations west and north-west of Kotelny Island were on open water and all other stations were under conditions of intense ice formation and ice thickness of 5 to 30 cm. On the Transdrift IV expedition, observations were made from fast ice up to 2.10 m thick. CTD-soundings were conducted using a sounding set OTS-PROBE Serie 3 (Meerestechnic Electronic GmBH, Germany).

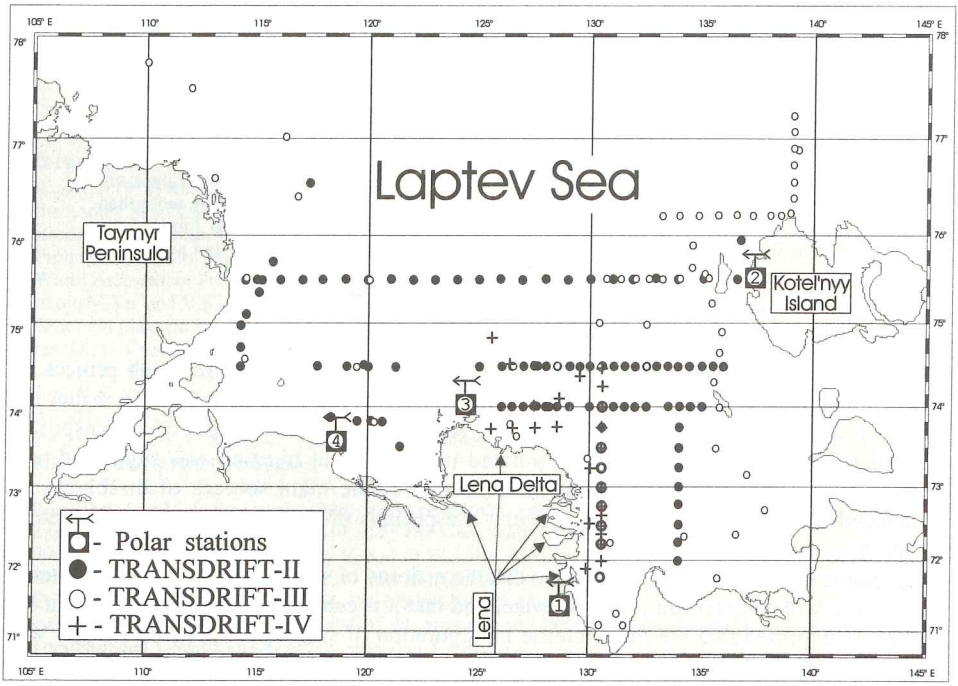

Figure 1: A scheme of the comprehensive oceanographic survey in the Transdrift II, Transdrift III and in the winter phase of the Transdrift IV expedition. Polar stations whose data were used: 1 - Tiksi, 2 - Kotel'ny, 3 - Dunai, 4 -Terpyai-Tumus.

The averaged daily data for standard meteorological air temperature observations at the polar stations "Kotelny", "Dunay", "Terpyai-Tumus", and "Tiksi" (Figure 1) were used for estimating the rate of ice formation in the winter season 1995-1996. The calculated values of ice thickness and salination were verified using CTD-data obtained at the same points in Transdrift IV expedition. The fast ice edge position was taken from the composite 10-day ice charts prepared in AARI on the basis of NOAA and METEOR satellite imagery.

The heat content of the water layers was calculated using actual CTD-data using the formula:

$$Q = \int_{h_1}^{h_2} C_p \rho (T_w - T_{fr}) dz \qquad (1)$$

where: C_p is heat capacity of sea water [J kg^{-1} °C^{-1}], ρ is sea water density [kg m^{-3}], h_1, h_2 are the lower and the upper boundaries of the water layer [m], T_w is water temperature [°C], and T_{fr} is the freezing point of the water [°C]. The formulae for calculating C_p, ρ, T_{fr} were taken from Fofonoff and Millard (1983). The integral in (1) was solved using the trapezoid formula. To obtain the specific heat content, the calculated values were normalized to the thickness of the corresponding layer.

Results

Comprehensive investigations in the summer of 1994 and autumn of 1995 resulted in a large body of information on the spatial and temporal (between summer to autumn) variations of hydrophysical properties within the zones of river water spreading.

The outflow situations in 1994 and 1995 differed considerably. In summer 1994, the outflow of river water was restricted to the south-eastern part of the sea (Figure 2A). In October 1995, the river outflow was spreading predominately towards the north-east (Figure 2B). Nevertheless, the outflow streams followed the sea bottom relief. The vertical salinity distribution in the river water outflow zones, in both 1994 and 1995, was characterized by the presence of two water layers that were vertically quasi-uniform. The upper layer was composed of freshwater, predominantly river discharge. The lower layer was Arctic bottom sea water. The upper quasi-layer was underlain by an intermediate slightly stratified water layer extending up to the main pycnocline. It was formed through the interaction between surface and bottom water. The intermediate water layer directly under the outflow channels was characterized by high concentrations of dissolved oxygen, chlorophyll *a* fluorescence, maximum values of the light transmission coefficient and minimum values of dissolved silicon (Dmitrenko et al., 1995; Golovin et al., 1995; Kassens and Dmitrenko, 1995; Kassens et al., 1997).

Calculations of the water heat content based on CTD-sounding data yielded the following results. The heat content of the intermediate water layer situated between the seasonal and the main pycnocline does not differ significantly from that of the upper well-heated quasi-uniform layer (Figure 3A) in the river water outflow zones during summer. In autumn, especially after the onset of ice formation, the heat content of the upper layer is actually zero. The heat content of the intermediate layer is much larger and remains relatively constant when compared to the summer season (Figure 3B). Hence, the thermal evolution of the water layer from summer to autumn in river discharge outflow zones can be represented as shown in Figure 3. The high heat content of the upper quasi-uniform layer is governed by radiation heating and wind and wave driven mixing in summer. However, the large heat content of the intermediate layer, given the strong density stratification at its upper boundary, requires a different explanation. The spatial variability of the water heat content in the intermediate layer was analyzed in the summer of 1994 and autumn of 1995 (Figure 4). If the heat content of the intermediate layer (Figure 4) is compared to the surface salinity distribution (Figure 2), it is evident that the distribution of higher heat content zones is determined by river water spreading. Regions with high intermediate layer heat content were located along the northern periphery of the spreading

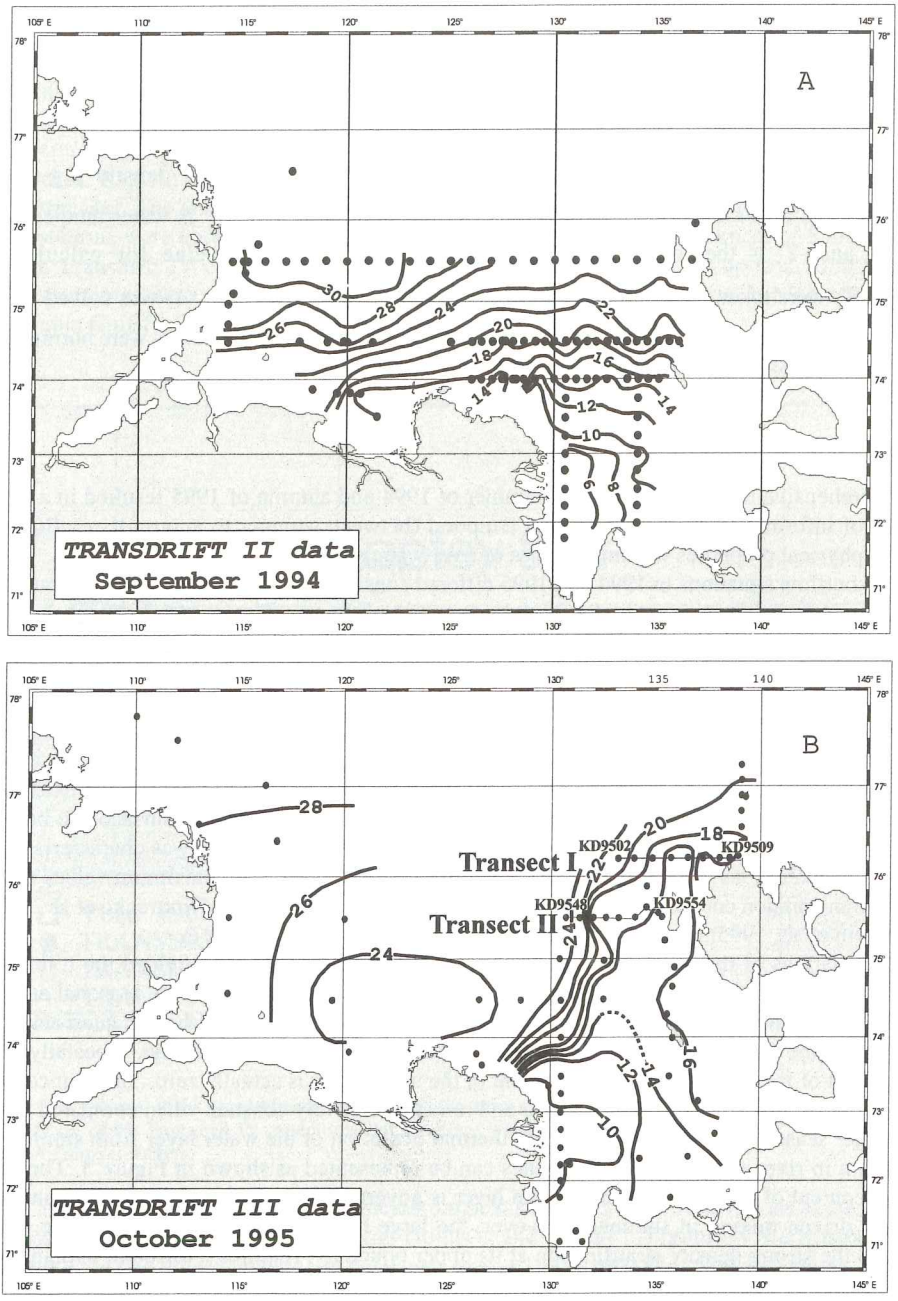

Figure 2: The surface salinity distribution in the Laptev Sea; September 1994, Transdrift II data (A) and October 1995, Transdrift III data (B).

river water. These results allow us to formulate the following questions:

- how is the warm intermediate water layer under the seasonal pycnocline formed?
- how does the intermediate water layer under the growing young ice (with a heat content comparable to that of the surface layer in summertime) influence the development of the winter ice and hydrological processes?

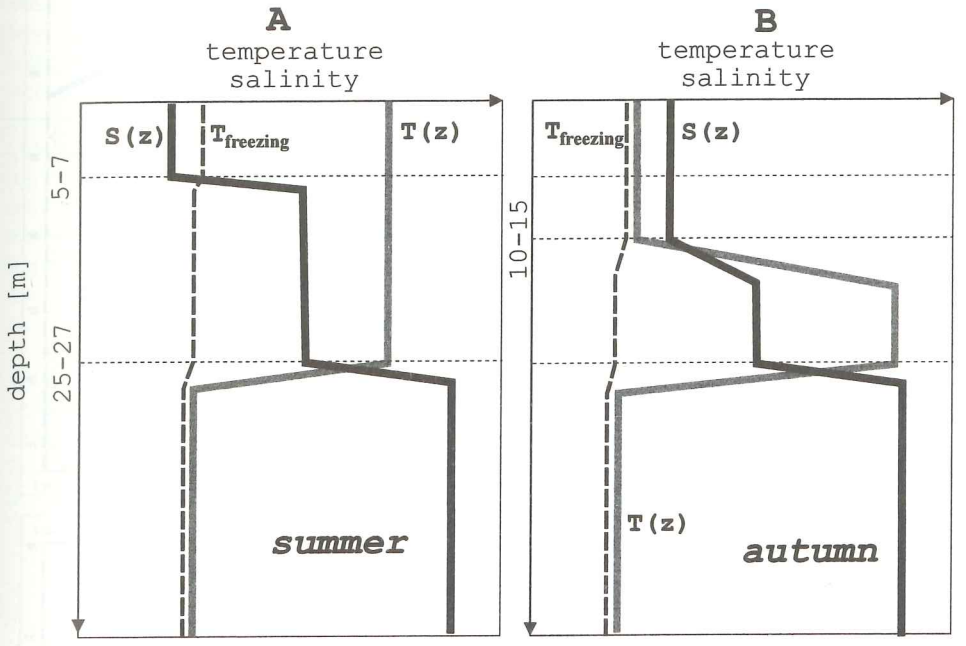

Figure 3: Typical evolution of thermohaline characteristics in the eastern Laptev Sea in the region of river discharge from summer (A) to autumn (B).

Frontal processes and the formation of the thermal subsurface layer

During spring and summer, the intensive river discharge to the Laptev Sea results in the formation of discharge hydrological fronts bounding the freshened water lens. Down to the depth of the discharge lens, the vertical isopycnals, isotherms and isohalines remain parallel to each other, intersected by equal pressure surfaces (baroclinic front; Figure 5A). Another type of front is formed in the lower quasi-isothermal water layer, especially at the periphery of the outflow zone between the seasonal and main pycnocline directly under the baroclinic front. The isopycnals and isohalines, which are approximately parallel to equal pressure surfaces, intersect the isotherms at an angle of up to 90° (Golovin et al., 1995). This is called the thermoclinic front (Figure 5A). The terms "baroclinicity" and "thermoclinicity" are used to indicate that isopycnic surfaces are intersected by equal pressure and temperature surfaces (Fedorov, 1991; Woods, 1980). Thus the discharge fronts in the Laptev Sea have a two-layer structure. From the surface to the depth of penetrating river water (seasonal pycnocline), they are baroclinic. In the lower layer, extending down to the main pycnocline, they are thermoclinic (Golovin et al., 1995). Two questions arise concerning the mechanisms of warm subsurface intermediate layer

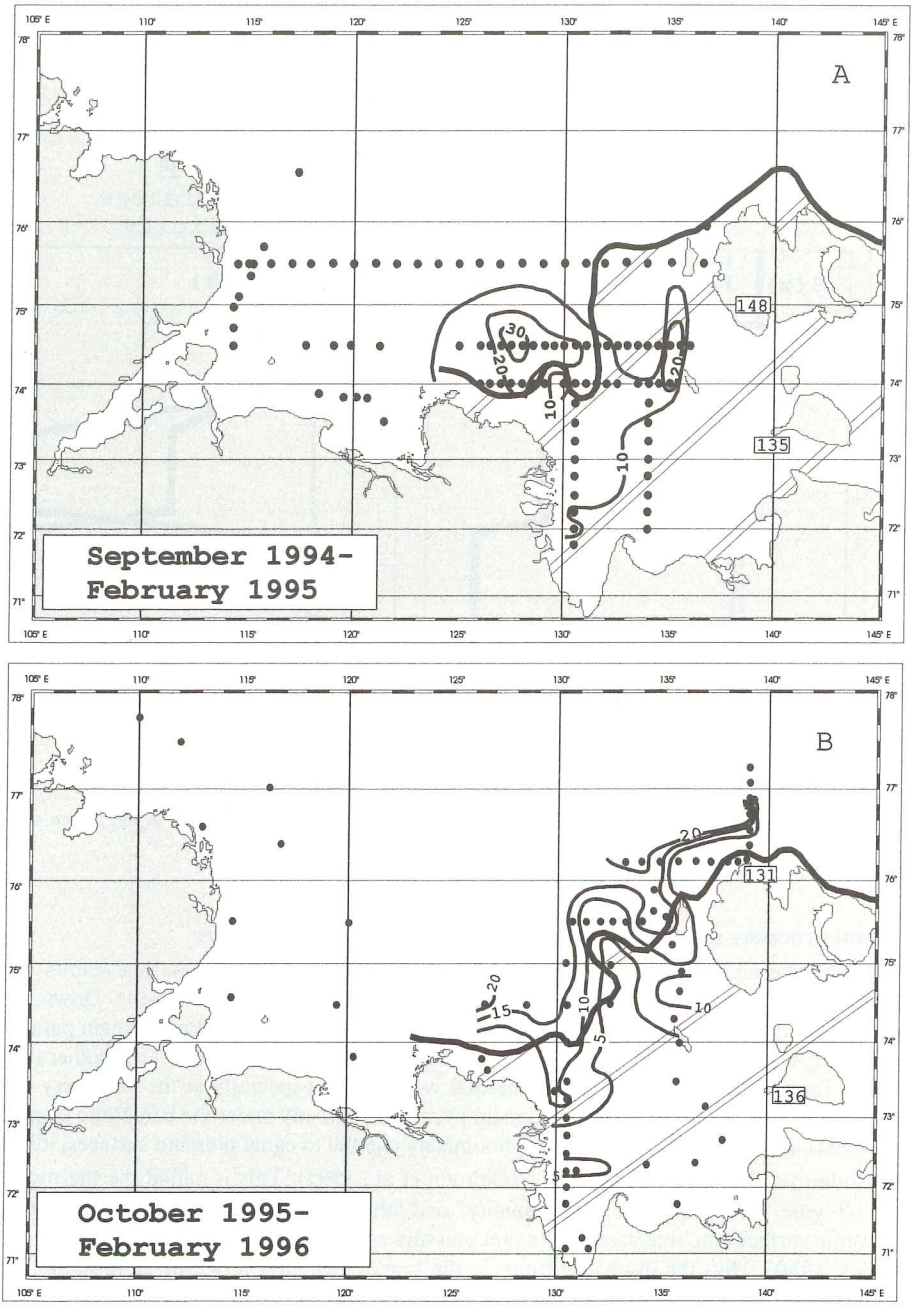

Figure 4: Spatial distribution of the heat content (in 10^4 KJ m^{-2}) of the intermediate water layer during September 1994 (Transdrift II data) (A) and October 1995 (Transdrift III data) (B) and a fragment of the composite ice chart for mid-February 1995 (A) and 1996 (B) (AARI data). ▬ - fast ice edge, ▨ - fast ice field, 123 - fast ice thickness, cm.

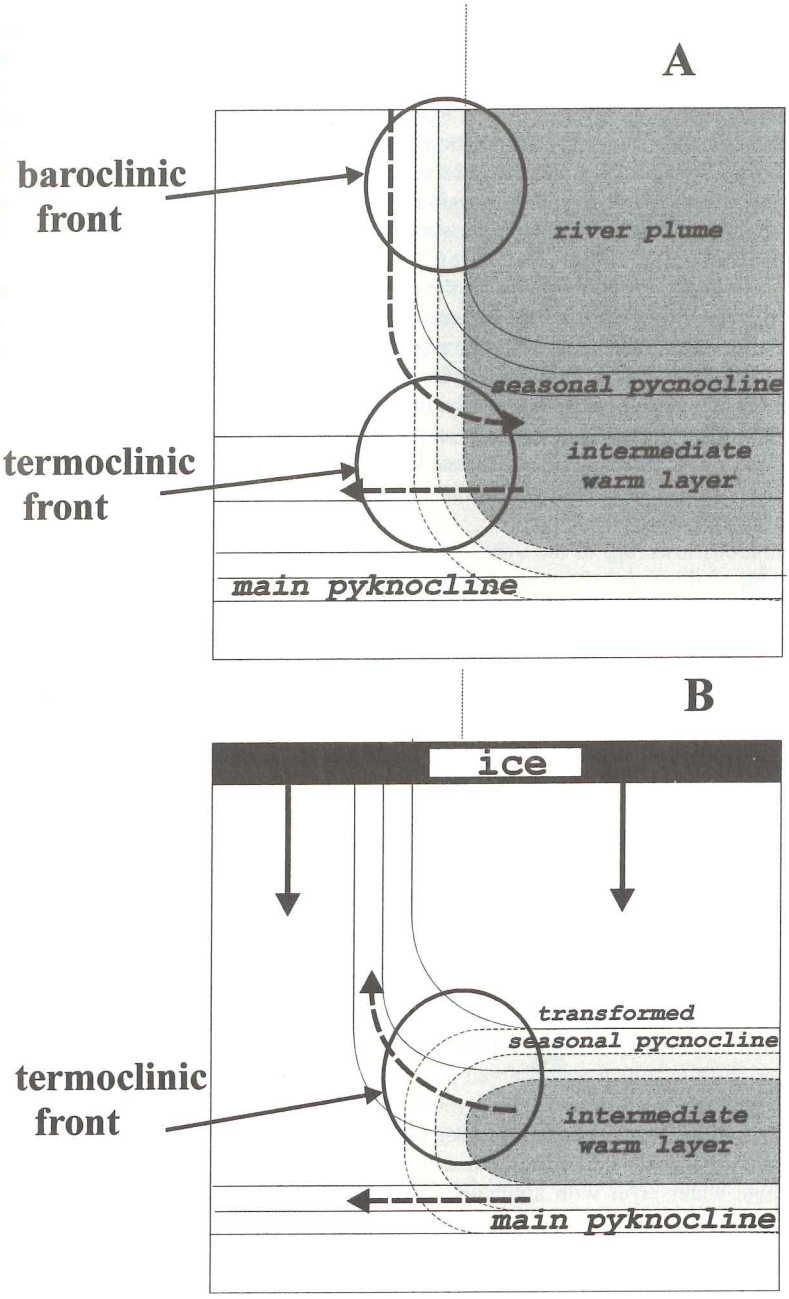

Figure 5: The structure of river discharge front and its evolution from summer (A) to winter (B). —— - isopycnals and isohalines, - - - - - - isotherms, ⟶ - salt flux, - - -▸ - heat flux.

formation: a) how do the discharge fronts spread to depths which exceed the depth of freshened water penetration by 4 to 5 times? and b) what mechanisms form the two-layer discharge

fronts? The most simple mechanism for the formation of the secondary thermoclinic discharge front relates to the isopycnic convergence of the solar-heated surface water beneath the river water lens. The lighter fresh water flows onto saline sea water. This mechanism is probably most important when the river discharge extends far northward from the river mouths. This must be accompanied by earlier ice melting in the same area in order for the water to have enough time to be heated (as occurred in the summer of 1995, for example). Obviously, the presence of a flaw polynya in these regions during winter and spring will increase heat accumulation (Zakharov, 1966), and thus warmer water will be "sucked" under the river water lens.

Another mechanism is connected with the possible deflection of the thermocline under the influence of frontal convergence in those cases when temperature does not influence the density field formation. This mechanism may be regarded as a passive admixture (Kuz'mina, 1980; MacVean and Woods, 1980). This process can be the most efficient when isotherms are initially inclined to isopycnals. This mechanism probably occurs within a short distance from the river mouth regions. It is most efficient during years when the main front-forming processes occur at a relatively small distance from the mouth regions (for example, the summer of 1994). Both mechanisms form the secondary thermoclinic front beneath the upper baroclinic one in the zone of frontal convergence.

An anomalous lowering of the upper well-heated quasi-thermal layer can result from the development of this type of convergence circulation at the front. The seasonal thermocline under the river water lens is located between 25 and 27 m, reaching the main pycnocline (Figure 3A), though its usual depth corresponds to the depth of the seasonal pycnocline (5-7 m). As the autumn progresses, radiative cooling, and wave and wind driven mixing occur, and the upper water layer is quickly cooled. However, a thicker heated water layer remains "buried" at depths of 10-12 to 25-27 m (Figures 3B, 5B). This leads to the generation of a thick anomalous warm water interlayer at the northern periphery of the zone of river water spreading during summer. Its stability in autumn results from the coincidence of the upper warm layer boundary with the position of the seasonal pycnocline.

A significant redistribution of oceanographic characteristics occurs under the influence of convergent processes in the region of the discharge fronts and under the lens of river water (Figure 6). The lowest concentration of dissolved silicon (less than 320 mg/l) was recorded in the intermediate layer directly under the outflow axes (Kassens and Dmitrenko, 1995; Kassens et al., 1997). In the surface and bottom layers, silicon concentration was 650 and 980 mg/l respectively. These layers coincided spatially with oxygen maxima, with enhanced chlorophyll *a* fluorescence, which reached values typical of the sea surface, and with the absolute maxima of the light transmission coefficients in water. These vertical distribution patterns typical of the river water outflow zone were observed both in summer 1994 and autumn 1995. It is obvious that water yielding such characteristics must originate at the surface. It is formed outside the river outflow zone (low values of dissolved silicon and high transparency). Then, as a result of frontal convergence in the spring and summer, it sinks, thus forming a sufficiently thick intermediate water layer with anomalous hydrochemical and hydro-optical characteristics (Figure 6).

Influence of the surface intermediate layer on the formation of ice-hydrological conditions in the autumn-winter season

The existence of a warm (up to 4°C) and thick (up to 20 m) water layer is expected to significantly alter ice formation conditions and subsequent ice growth processes in regions affected by river discharge. The heat flux from this layer to the surface can probably limit ice

formation via convection and may to some extent govern the position of the fast ice edge and the flaw polynya, presumably through some efficient mode of heat transfer to the surface.

Figure 4 provides a basis for testing for a correlation between the fast ice edge position and the heat content of the subsurface layer at a time when the edge position was quasi-steady (mid-February 1995 and 1996). Clearly, fast ice in the eastern Laptev Sea was stable during the autumn of 1994 and was congruent with the spread of river water and with heat content isolines for the subsurface layer (Figure 4A). Fast ice edge formation during the 1995-1996 autumn and winter seasons displayed similar congruencies: the configuration of the fast ice edge correlates well with the heat content isolines in the intermediate layer (Figure 4B). Thus, it seems that the quasi-steady position of the fast ice edge depends on the heat supply from the intermediate water layer. In the river water discharge zones, the fast ice edge was located much further south (up to 150 km) than the northern boundary of river water spreading. Analysis of weekly ice charts has shown that the northward spreading of fast ice was in agreement with the heat content of the intermediate water layer. Investigations of the annual variability of the mid-winter fast ice edge position between 1990 and 1996 shows that it is governed to some extent by the direction of river water spreading in the preceding summer season.

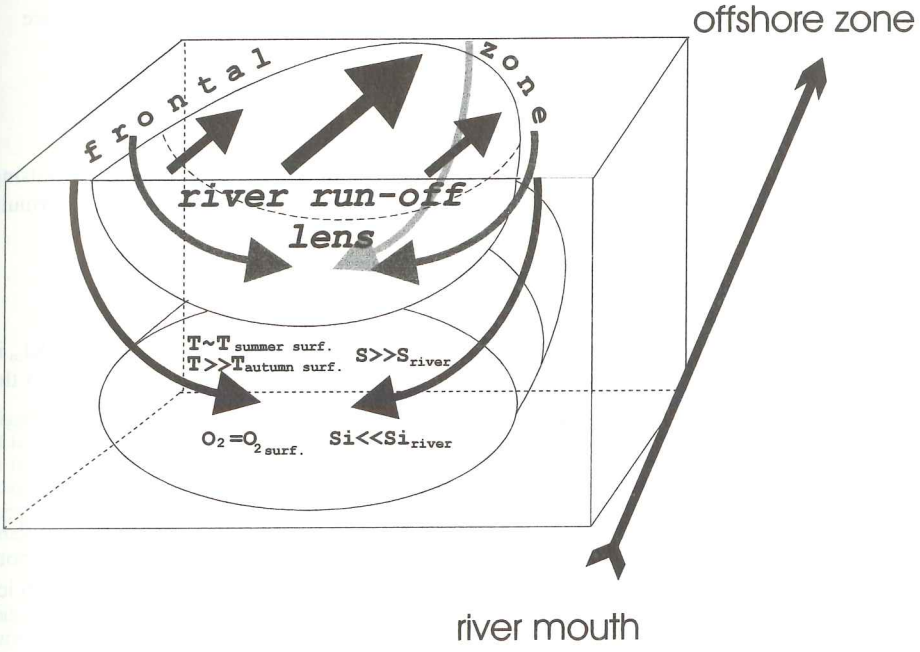

Figure 6: A scheme of the frontal convergence at the discharge hydrofronts; ⟶, direction of convergent motions, ⟶, direction of river water spreading.

The features mentioned above suggest that there exist mechanisms for heat exchange between the intermediate layer and the water surface under the ice cover. The incoming heat restricts ice formation and thus directly influences ice formation conditions. Let us assume that the heat content of the intermediate water layer is $20 \cdot 10^4$ KJ m^{-2} (data from the Transdrift III expedition), the mean salinity of the ice core is 4 (Transdrift IV expedition), and the ice temperature is -2°C at the ice-water boundary and -25°C at the ice-air boundary. Ice core temperature distribution is considered to be linear (Doronin and Kheisin, 1975). According to

Oceanographic Tables (1975), if all heat from the intermediate layer is transferred to the surface, the sea ice core growth is reduced by 68 cm. Is this sufficient to control the ice conditions to the extent as shown in Figure 4? Observations carried out on the ESARI-92 expedition in the eastern Laptev Sea showed that the thickness of fast ice in the vicinity of the fast ice edge was about 1.9 m (Dethleff et al., 1993). This value differs from the thickness of the first-year drifting ice behind the flaw polynya by a value of the same magnitude.

As follows from Figure 4, by the time the fast ice edge attained a quasi-steady character, its position was to a great extent governed by the heat content of the intermediate water layer. If this is the case, then there must have been some mechanisms for an extremely effective heat exchange with the surface. Let us discuss the entire complex of mechanisms responsible for heat transfer from the intermediate warm layer to the lower ice boundary.

Theoretical considerations suggest that the heat exchange between the lower ice surface and the warm intermediate layer, limited by the seasonal pycnocline from above and by the main pycnocline from below, can via the following:

- molecular heat exchange;
- turbulent heat exchange;
- convective heat exchange caused by salination of the surface layer at ice formation;
- double-diffusion convection through the seasonal pycnocline with the surface sub-ice layer;
- intrusion stratification through the lateral boundaries of the thermocline front.

Molecular heat exchange

The molecular heat fluxes calculated during the onset of ice formation in autumn of 1996 using TRANSDRIFT III data vary within 0.1 - 0.5 J $m^{-2} \cdot s^{-1}$. For this calculation, a simple formula (2) has been used (Turner, 1973):

$$Ft_m = Kt_m \cdot DT/DZ, \qquad (2)$$

where DT is the temperature difference through the pycnocline with a thickness DZ, and Kt_m is the coefficient of molecular temperature conductivity ($1.3 \cdot 10^{-7}$ m^2 s^{-1} for sea water). In the mass form the heat flux can be presented as:

$$Q_m = Ft_m \cdot r \cdot Cp \qquad (3)$$

where r is the sea water density and Cp is the heat capacity of sea water (approximately 4.19 $J \cdot g$ $°C^{-1}$. In the three months during which the fast ice edge becomes quasi-steady, about $2.26 \cdot 10^{-3}$ to $21.60 \cdot 10^{-3}$ KJ m^{-2} are transferred to the upper layer. This leads to a decrease in ice thickness of 2 to 7 cm (process 1, Figure 7).

Turbulent heat exchange

The criterion for different regimes of turbulent exchange is the Richardson gradient number. For polar regions, it can be written in the form

$$Ri = g \cdot bDS \cdot H_P \cdot DU^{-2} \qquad (4)$$

where g is gravitational acceleration, $DU \cdot H_P^{-1}$ is the gradient of the horizontal component of the current speed in the pycnocline, DS is the salinity difference in the seasonal pycnocline and b is the salinity compression coefficient. Calculations of the Richardson gradient number for the seasonal pycnocline presented in Table 1 were made for the stations on transect II (Transdrift

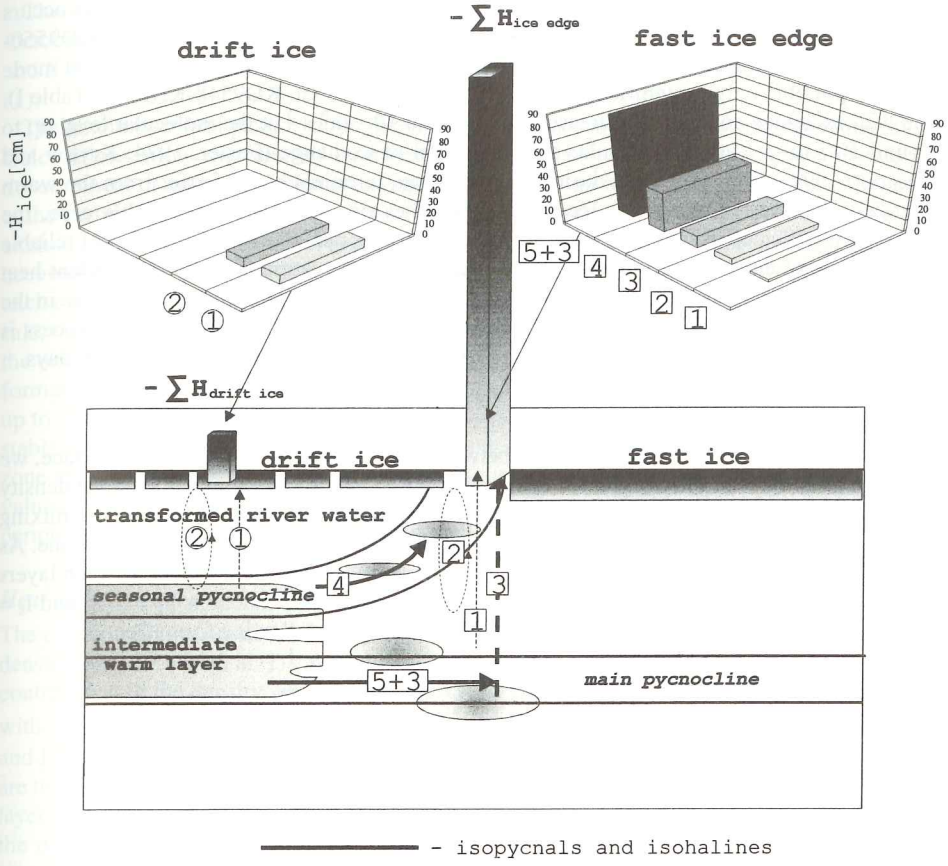

Figure 7: A scheme of the influence of the heat fluxes from the intermediate layer to the surface on the formation of ice conditions in the zone of river water spreading. 1 - molecular heat exchange, 2 - convective heat exchange at ice formation, 3 - double-diffusion convective heat exchange, 4 - heat exchange governed by isopycnic advection of intrusions to the surface, 5+3 - heat exchange governed by the double-diffusion convection at the upper periphery of isopycnic intrusions. The upper diagrams present the efficiency of each of the enumerated processes calculated to centimeters of ungrown ice.

Table 1: Estimates of the Richardson gradient number for different shear values for the horizontal component of current speed (Transdrift III, transect II data).

Station (KD95..)	48	49	50	51	52	53	55	54
DS	7.2	7.7	13.3	11.8	12.9	13.7	14.2	13.2
DU=2 cm/s	619	409	1121	1022	1194	2230	1858	5804
DU=15 cm/s	11	7	20	18	20	40	103	33

III) across the zone of river water spreading (Figure 2B). These estimates were based on the data collected by oceanographic stations during the onset of intensive ice formation and were

calculated for two speed shear values. As a rule, exchange through the density boundary occurs at the molecular scale even at DU = 15 cm/s: Ri>15, (Narimousa et al., 1986; st. KD9550-KD9554, Table 1). Heat exchange through the pycnocline via this molecular-turbulent mode becomes possible only at significant shear speeds: 1.5<Ri<15 (st. KD9548-KD9549, Table I). The heat exchange coefficient increases from around 10^{-7} m^2 s^{-2} at the molecular level up to around 10^{-4} m^2 s^{-1} at the molecular-turbulent level of exchange (Foster, 1974; Krylov and Zatsepin, 1992). With salination during ice formation, turbulent heat transfer from the warm intermediate layer to the lower ice surface becomes possible (Ri<1.5). In this case, the exchange coefficient can increase up to about 10 m^2 s^{-1} (Foster, 1974). The absence of reliable observations of currents during autumn and winter prevents estimation of the turbulent heat exchange efficiency. However, it should be noted that in spite of the significant increase in the efficiency of the heat exchange at the turbulent-molecular and turbulent scales, the process is only of a local and occasional character. It is hardly effective at time scales of about 100 days.

Convective heat exchange

To estimate the convective heat exchange between the intermediate layer and the surface, we followed Zubov,s method (Zubov, 1963), which is based on the supposition that, at the density of the upper expanding layer, the stratification tends to become stable. This results in mixing that penetrates to the depth at which the upper layer density is equal to that of the lower one. As this takes place, the heat accumulated by the lower layer is equally redistributed between layers involved in mixing. Calculations of discrete approximations of the functions $S_k = S(I_k)$ and $I_k = I(H,S)$ for the stage of salinity convection were made using the following formulae:

$$I_k = \sum_{i=1}^{k} \frac{1.1(H_{i-1} - H_i)\cdot(S_{i-1} - S_i)}{S_{i-1}} \qquad (5)$$

$$S_k = f(\rho_k, T_w) \qquad (6)$$

$$\rho_k = \sum_{i=2}^{k} \left(\frac{\sum_{m=1}^{i-1} \rho_m}{2^{i-1}} + \frac{\rho_i}{2}\right) \qquad (7)$$

$$H_k = H(I_k) \qquad (8)$$

where i is the level number from the sea surface in CTD-sounding; k is the level up to which the convective mixing spreads; H_i, S_i, r_i are the depth, salinity and density at level i; H_k is the depth of convection penetration during spreading up to the level k; S_k and r_k are salinity and density of the convectively mixed layer; I_k is the ice thickness increase sufficient for convection penetration up to level k; T_w is the water's freezing temperature at a given salinity; the function f is the equation of sea water state solved numerically relative to salinity by the method of successive approximations.

Salinity, temperature and the depth of the convective mixing layer were selected by means of the discrete analogue of functions S_k, T_k, $H_k = F(I_k)$ calculated from formulas (5) - (8) and from the "actual" ice thicknesses obtained from Zubov's empirical formula (9) (Doronin and Kheisin, 1975; Zubov, 1963):

$$I_k = -25 + [\,(25 + I_0)^2 + 8S(-T)\,]^{1/2} \qquad (9)$$

The sum of freezing degree-days S(-T) was calculated using mean daily air temperature from October to June 1994-1995 and 1995-1996 at the polar stations Terpyai-Tumus, Dunai, Tiksi, and Kotel'nyy (Figure 1). The convective heat exchange was estimated using the ratio given in (1).

The amounts of heat passing through the surface due to convective processes are rather small. Calculations show that density stratification in the river water outflow zone prevents the development of convective heat exchange (st. KD9502 and KD9503 in Figure 8A). However, at the periphery of the outflow zone, where density stratification is weaker, the convective heat exchange becomes much more efficient. In the outflow zone, about 10% of the heat accumulated in the intermediate layer can be transferred to the surface due to convective heat exchange. At the periphery, this value increases up to 40-60% (st. KD9504 in Figure 8A). As a rule, the convective heat exchange is more efficient at the beginning of the winter season up to the time the fast ice edge becomes quasi-steady. On average, during the first three months of ice formation, the amount of transferred heat is four times as large as during the next four months up to the time the ice growth ends (Figure 8A, position I, II). When the fast ice edge becomes stable, the ice growth is reduced by 27 and 7 cm at the periphery of the river water outflow zone and beneath it, respectively (process 2, Figure 7). At the time the ice growth ends, these values increase by 15 and 3 cm, respectively. On average, these values are even less at the periphery of the outflow zone and do not exceed 10 cm at the time the ice edge becomes stable.

Heat exchange governed by double-diffusion

The criterion for the possible occurrence of double-diffusion convection is a certain value of the density ratio, $Rr = bDS \cdot aDT^{-1}$, for the density boundary, where temperature makes an unsteady contribution to the density gradient. Here $b = 8 \cdot 10^{-4}$ is the coefficient of salinity compression, with dimensions inverse to salinity, $a = 7 \cdot 10^{-5}$ [°C^{-1}] is the temperature expansion coefficient, and DT and DS are the salinity and temperature differences at the boundary. In our case, these are the temperature and salinity differences across the upper boundary of the warm intermediate layer (the upper part of the seasonal pycnocline). It was found that Rr = 15 is the upper limit for the development of double-diffusion convection and accompanying step-like thermohaline structures (Fedorov, 1976; Huppert, 1971; Neshyba et al., 1971). At Rr > 15, exchange through the boundary surface becomes purely molecular. Estimates of the actual density ratio at the upper boundary of the seasonal halocline at the time preceding ice formation, Rr (only for transect I); at the beginning of ice formation, Rr_f; and at the time the fast ice edge becomes quasi-steady, Rr_i, are presented in Table 2. To calculate the density ratio, Rr_i, the thermohaline characteristics of the upper sub-ice layer calculated using formulae (4) - (8) were used.

Our estimates show that double-diffusion convection before ice formation is impossible (st. KD9502-KD9509, Table 2). During the initial period of ice formation, the double-diffusion convection is possible only at the periphery of the river outflow (st. KD9505, KD9548 in Table 2). When the fast ice edge becomes quasi-steady, the area expands (st. KD9502, KD9503, KD9505, KD9507, KD9509, KD9548, KD9549). However, in the central part of the river outflow zone, the double-diffusion is either extreme or absent during the entire winter season due to the high stability of the seasonal pycnocline.

The heat exchange values governed by double-diffusion have been calculated using a ratio obtained experimentally by Turner (1965, 1973). Based on the Turner´s experiments, Huppert (1971) suggested a formula for calculating the convective heat flux which expresses the dependence of this flux on the Rr value:

$$Ft = b \cdot Ft^{*} \cdot Rr^{-2}, \qquad (10)$$

where b = 3.8, and Ft^* is the heat flux through the boundary at a given temperature difference, DT, which is determined in Fedorov (1976) as:

$$Ft^* = 0.085\ (g \cdot a \cdot Kt_m^2/n)^{1/3} \cdot (DT)^{4/3} = g_m \cdot (DT)^{4/3}, \quad (11)$$

where Kt_m is the coefficient of molecular temperature conductivity, n is the kinematic coefficient of molecular viscosity, and g is gravitational acceleration. It follows from (10) and (11) that:

$$Ft = b \cdot g_m \cdot (DT)^{4/3} \cdot Rr^{-2} \quad (12)$$

Formula (12) has been used to estimate the heat fluxes when Rr<15.

Table 2: Estimates of the density ratio in the inversion area of the warm intermediate layer along transects I and II of the Transdrift III expedition.

Station (KD95..)	02	03	04	05	06	07	08	09
Rr	32.0	56.1	45.0	-	88.5	43.3	92.3	34.2
Rr_f	13.8	23.3	22.6	5.0	23.7	5.7	40.1	12.0
Rr_i	15.8	16.9	19.4	3.9	18.6	1.3	37.0	6.5
Station (KD95..)	48	49	50	51	52	53	55	54
Rr_f	13.4	22.7	63.4	92.8	42.9	29.4	46.7	27.6
Rr_i	2.2	11.3	43.6	64.1	27.9	20.1	35.3	21.1

Figure 8B, position I, presents the heat exchange values calculated from ratio (12) during the transition to a quasi-steady fast ice edge (transect I, Transdrift III expedition). Calculations were performed for the density ratios, Rr_f, which corresponded to the initial stage of ice formation. Actually, they represent the lower estimate of the possible heat exchange values for this period. The upper estimate corresponds to the value of the density ratio, Rr_i (position III, Figure 8B). On average, the latter is 1.5-2 times greater. But at the periphery of the river water outflow zone, double diffusion convection is capable of not only "transferring" practically all heat - the potential heat transfer is 5-20 times greater than the actual transfer (st. KD9505, KD9507 in Figure 8B, position III). Taking the periphery stations KD9507 and KD9548 as an example, by February 10th the upper estimates of the heat which can be transferred from the intermediate layer to the surface are 20 times larger than the lower estimates ($520 \cdot 10^4$ and $246 \cdot 10^4$ KJ/m^2, respectively). For the assumed ice cover characteristics, the actual ice growth at the periphery of the outflow zone is reduced by 20 cm when the fast ice edge becomes stable (process 3, Figure 7). The potential ice growth in the presence of a continuous heat flux is reduced by 84 cm (lower estimate). The upper estimates of the same values are 44 and 130 cm, respectively.

Let us draw some conclusions. For the strong density stratification observed in the river water outflow zone, the convective heat transfer is comparable to the molecular processes. Since double-diffusion is impossible in these regions, only these two processes, with an

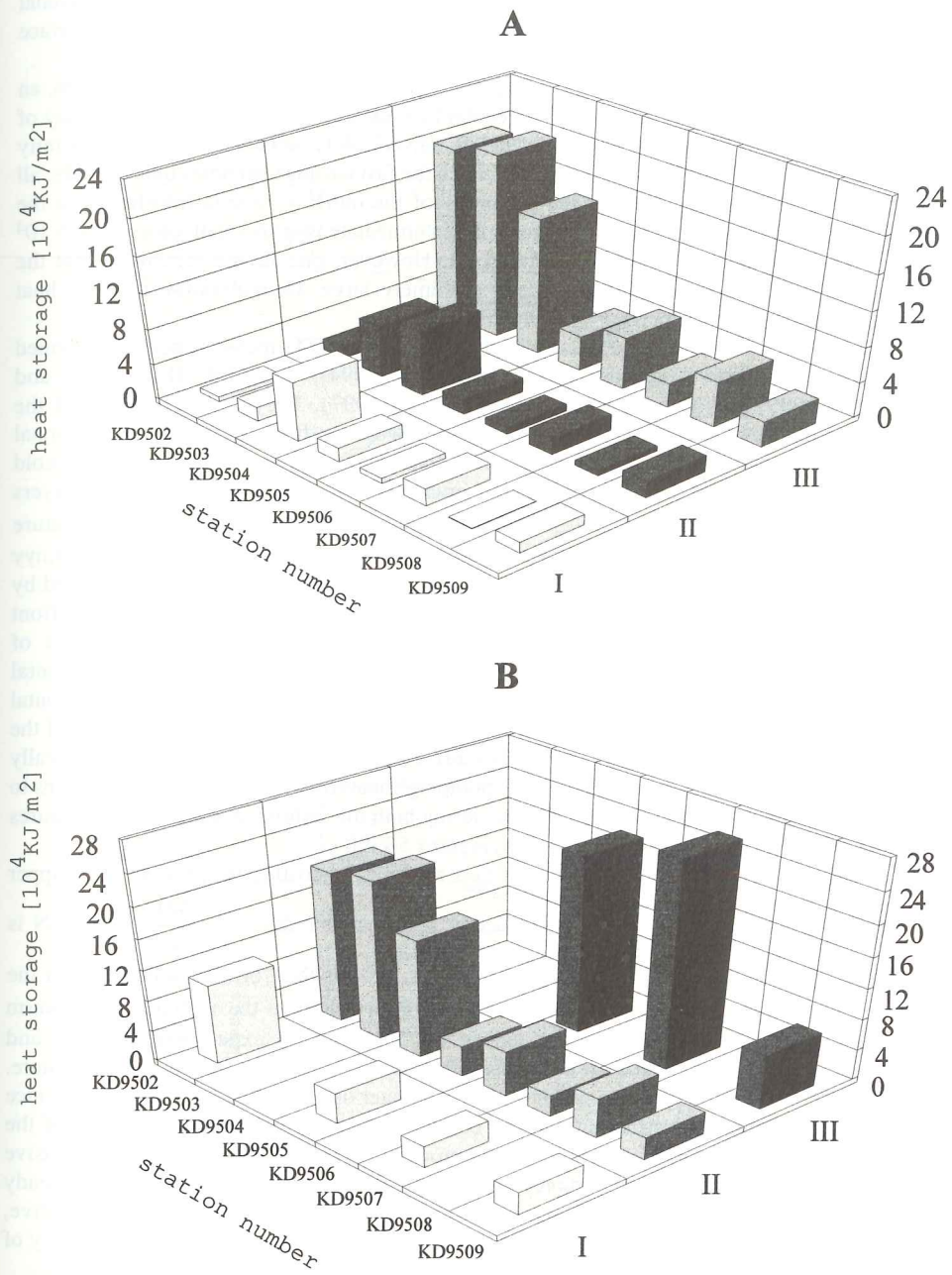

Figure 8: The amount of heat transferred to the surface from the intermediate layer due to both convection at ice formation (A) and double-diffusion convection (B), transect I of the Transdrift III expedition. A: I - by the time the fast ice edge attains a quasi-steady character, II - by the time the ice growth ends, III - the total heat supply of the intermediate water layer; B: I - by the time the fast ice edge attains a quasi-steady character (lower estimate), II- the total heat supply of the intermediate water layer, III - the upper estimate of a potential transfer.

insignificant contribution from the turbulent heat transfer, govern heat flux through the seasonal pycnocline to the surface (Figure 7, left diagram). The amount of heat transferred to the surface by these processes cannot influence the ice cover formation to the extent shown in Figure 4.

At the periphery of the outflow zone, convection is usually 5 times (and, as a maximum, an order of magnitude) more efficient than molecular heat exchange. However, the efficiency of the heat exchange governed by double-diffusion convection is twice as large as the salinity convection (right diagram, Figure 7). So, even when the fast ice edge becomes quasi-steady, all heat from the intermediate layer at the periphery of the outflow zone is transferred to the surface. In reality, however, the heat flux from the intermediate layer is small, on average $5 \cdot 10^4$ KJ m^{-2}, *i.e.* equivalent to 16 cm of unformed ice. However, one should remember that the potential heat exchange with the surface is extremely large. Its realization requires heat advection from the adjacent parts of the river discharge zone.

The existence of such advection was tested by numerous CTD-measurements performed during the expeditions Transdrift I (Kassens et al., 1994), Transdrift II (Kassens and Dmitrenko, 1995) and Transdrift III (Kassens et al., 1997). They demonstrated that the temperature distribution at the periphery of the river water outflow zone under the seasonal pycnocline was characterized by numerous inversions. The thickness of such warm and cold interlayers reached 10 m, and the temperature gradients at the boundaries of the interlayers reached 2-2.5 °C m^{-1} (Golovin et al., 1995). The most pronounced isopycnic temperature inversions were observed at the periphery of the freshened zone in the region west of Kotel,nyy Island during the autumn of 1995 (Figures 1, 9). Their formation was shown to be caused by the existence of the secondary thermoclinic front under the baroclinic surface discharge front (Golovin et al., 1995; Kassens and Dmitrenko, 1995; Figure 5). The mechanisms of thermoclinic front formation were considered in Discussion I. In the absence of horizontal density stratification, but in the presence of strong temperature stratification, any horizontal disturbance leads to the formation of intrusions. It is obvious that intrusion stratification of the thermoclinic secondary hydrofront and further advection of heat transferred by isopycnically spreading warm intrusions are the processes "pumping" heat from beneath the discharge lens to its periphery. This process is equally efficient during both the summer-autumn season (Figures 5A, 9A) and the period of young ice growth (Figures 5B, 9B).

The formation of intrusions at the front is a typically ageostrophic process. The upper estimate of its spatial scale is the Rossby baroclinic deformation radius: $\lambda = \frac{ND_0}{\pi f}$, where N is the Vaisala frequency, D_0 is the fluid layer thickness, and f is the Coriolis parameter. For the Laptev Sea, we have estimated λ=11.8 km. Actual observations of the spatial scale of warm intrusions near the thermoclinic front during the Transdrift II expedition (Kassens and Dmitrenko, 1995) showed that their horizontal dimensions could reach 4 kilometers and more. This estimate is comparable to the width of the river water outflow zone (about 150 km), since the process of intrusive destruction goes on continuously until complete degradation of the warm water layer. The high efficiency of this process permits the assumption that intrusive destruction of the warm layer is complete by the time the fast ice edge attains a quasi-steady character. All heat except for the heat already transferred to the surface via convective, turbulent, and molecular heat exchanges will be redistributed by advection to the periphery of the outflow zone.

Figure 5 displays the evolution of the outflow front from summer (A) to winter (B). Salination of the surface layer occurs at ice formation. As a result, some heat from the upper part of the intermediate layer can be isopycnically exchanged with the surface (Figure 5B, Figure 7, process 4). In order to estimate the intensity of this type of heat exchange, we used the ratios (1), (5) - (9) for the time during which the fast ice edge stabilizes. When calculating,

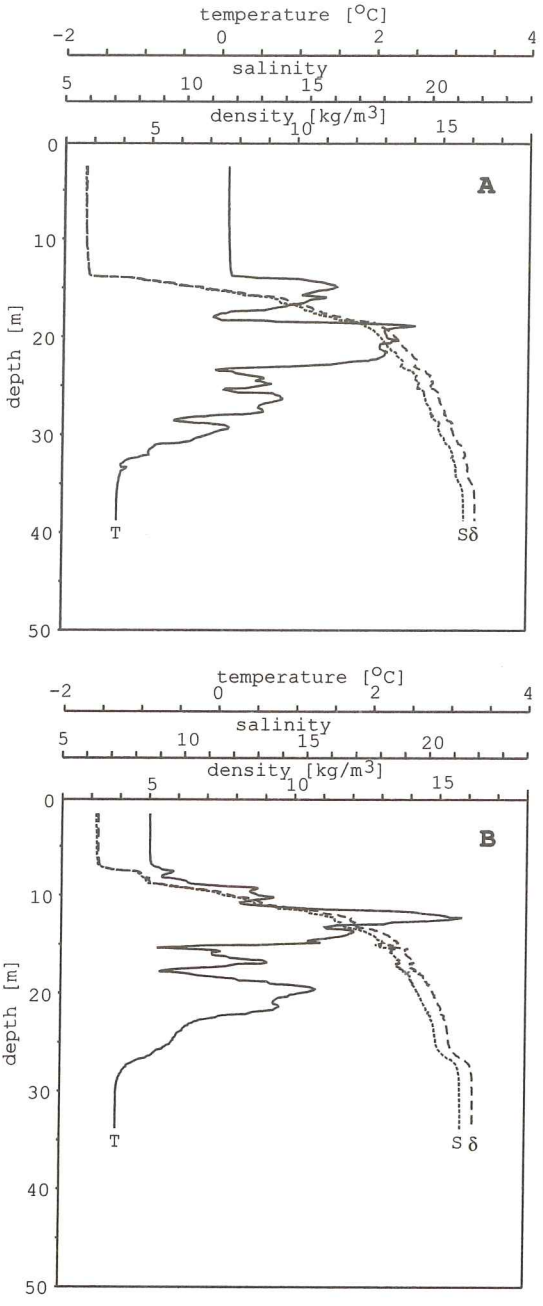

Figure 9: Vertical distribution of thermohaline characteristics at stations KD9519 in open water (A) and KD9554 under the young ice up to 25 cm thick (B).

we assumed the average advection rate to be 4 cm s^{-1}. It was also assumed that advection occurs in all directions with equal probability. It has been established that up to 25% of heat accumulated in the intermediate layer under the lens of freshened water can be transferred directly to the surface by the time the fast ice edge becomes quasi-steady at the periphery of the outflow zone. This results in a concentration of heat in the peripheral zone. The cumulative effect of all vertical heat exchanges with the intermediate layer (in the regions of the peripheral zone itself) amounts to, on average, $15 \cdot 10^4$ KJ m^{-2}. This is equivalent to 47 cm of unformed ice. The amount of heat transferred to the surface by isopycnic advection is twice as large as the amount transferred to the surface via vertical heat exchange.

The heat which remained in the intermediate layer after vertical and quasi-horizontal heat exchange was isopycnically transferred by horizontal advection beneath the periphery of the freshened water zone. Here the double-diffusion heat exchange processes are extremely efficient. Let us assume that, as shown above, the complete destruction of the intermediate warm layer via intrusive stratification occurs even prior to the fast ice edge becoming quasi-steady. Then the heat concentration beneath the periphery of the freshened zone can reach $26 \cdot 10^4$ KJ m^{-2} and more. This corresponds approximately to the lower estimate of the possibility of a double-diffusion heat transfer to the surface (process 5+3, Figure 7). The upper estimate was, as we recall, an order of magnitude greater.

The total heat transfer to the surface can reach $41 \cdot 10^4$ KJ m^{-2} and more by the time the fast ice edge becomes quasi-steady due to all acting processes: molecular and turbulent heat exchange, salinity convection, double-diffusion, "quasi-horizontal" advection of warm intrusions to the surface, horizontal advection of warm intrusions with "secondary" double-diffusion. This would be equal to 129 cm of unformed ice (Figure 7). It is thus not surprising that, in the three months after the onset of ice formation, the fast ice edge already becomes quasi-steady precisely at the periphery of the zone freshened by river discharge.

Conclusions

Figure 7 presents a scheme that summarizes the possible heat exchange mechanisms between the intermediate warm layer and the lower ice boundary. The diagrams above the scheme present the estimates of heat exchange efficiency in cm of unformed ice for all processes under study. A comparison with the actual observed ice cover types confirms our suggestions and provides justification for the following conclusions.

1 Formation of the fast ice edge in the eastern Laptev Sea depends to a great extent on processes determined by the spreading of river discharge. The quasi-steady position of the fast ice edge is confined to the periphery of the transformed river water spreading, and is governed by the large intensity of the heat exchange in this zone.
2 The fast ice edge is formed much further southward than the northern limit of the river discharge spreading. River water rich in suspended matter is located within the zone of drifting ice and the flaw polynya. Its incorporation into drifting ice intensively produced in the polynya triggers a complex of processes usually referred to as the "Transarctic ice transport of river discharge".

Acknowledgements

This article is one result of 4 years of research and expedition studies under the Russian-German Project "Laptev Sea System". The work of many Russian and German scientists in various disciplines of natural science served as a basis for obtaining the results; the authors express their most sincere gratitude to all of them. The results presented here could not have

been obtained without the selfless work, under heavy weather and difficult ice conditions, of the crews of the R/V "Professor Multanovsky", the icebreaker "Kapitan Dranitsyn" and their captains, V. Danilenko and O. Agofonov, and the MI-8 helicopter crews of the Tiksi Joint Air Team headed by I. Litovchenko. The authors are grateful to all these people for their fruitful work. Much of this article was initiated and written by the Russian and German authors in 1995 and 1996 in GEOMAR, Kiel. The authors gratefully acknowledge assistance of the German Ministry of Education, Science, Research and Technology (BMBF Grant No. 525 4003 0G0517A). The Russian contribution was also supported by the Russian Ministry for Science and Technical Policy (LAPEX). The authors greatly appreciate the help of the Russian and German scientific coordinators of the project "Laptev Sea System" - Prof. J. Thiede and Prof. L. Timokhov, whose attentive and friendly attitude has enabled the authors to successfully fulfill these studies. Special thanks are due to Dr. V. Zelensky, Head of the Tiksi Territorial Administration for Hydrometeorology for providing meteorological information used in the article and Dr. V. Grishenko, Deputy Director of the AARI for the composite ice charts required for this study. The English manuscript was kindly improved by Pier Paul Overduin.

References

Dethleff, D., D. Nürnberg, E. Reimnitz, M. Saarso and Y.P. Savchenko (1993) East Siberian Arctic Region Expedition ,92: The Laptev Sea - Its Significance for Arctic Sea ice Formation and Transpolar Sediment Flux. Ber. Polarforsch., 120, 1-44.

Dmitrenko, I. and TRANSDRIFT Shipboard Scientific Party (1995) The Distribution of River Run-Off in the Laptev Sea: The Environmental effect. In: Russian-German Cooperation: Laptev Sea System, Kassens, H., D. Piepenburg, J. Thiede, L. Timokhov, H.-W. Hubberten and S. Priamikov (eds.), Ber. Polarforsch. 176, 114-120.

Dmitrenko, I, J. Dehn, P. Golovin, H. Kassens and A. Zatsepin (in press) Influence of sea ice on under-ice mixing under stratified conditions: potential impacts on particle distribution. Estuarine, Coastal and Shelf Science, 46.

Doronin, Y.P. and D.E. Kheisin (1975) Sea Ice (in Russian). Gidrometeoizdat, Leningrad, 317 pp.

Eicken H., E. Reimnitz, V. Alexandrov, T. Martin, H. Kassens and T. Viehoff (1997) Sea-ice processes in the Laptev Sea and their importance for sediment export, Continental Shelf Research, 17, 205-233.

Golovin, P.N., V.A. Gribanov and I.A. Dmitrenko (1995) Macro- and Mesoscale Hydrophisical Structure of the Outflow Zone of the Lena River Water to the Laptev Sea. In: Russian-German Cooperation: Laptev Sea System, Kassens, H., D. Piepenburg, J. Thiede, L. Timokhov, H.-W. Hubberten and S. Priamikov (eds.), Ber. Polarforsch. 176, 99-106.

Fedorov, K.N. (1976) Fine Thermohaline Structure of the Oceanic Waters (in Russian). Leningrad, Gidrometeoizdat, 184 pp.

Fedorov, K.N. (1991) About Thermohaline Characterisrics of Oceanic Fronts (in Russian). In: K.N. Fedorov. Izbrannye Trudy po Fizicheskoi Okeanologii, Gidrometeoizdat, Leningrad, 106-111.

Fofonoff, N.P. and R.C.Jr. Millard (1983) Algorithms for computation of fundamental properties of seawater. Unesco technical paper in marine science, 44, 53 pp.

Foster, T. D. (1974) Thi hierarchy of convection. In: Processus de formation des eaux oceaniques profondes en particulier en Mediterranee Occidentale, Colloques Intern., du CNRS, Paris, 215, 237.

Huppert, H.E. (1971) On the stability of double-diffusive layers. Deep-Sea Res., 18, 10, 1005-1022.

Kassens, H. & I. Dmitrenko (1995) The TRANSDRIFT II Expedition to the Laptev Sea. In: Laptev Sea System: Expeditions in 1994, Kassens H. (ed.), Ber. Polarforsch. 182, 1-180.

Kassens, H., V. Karpiy (eds.) and the Shipboard Scientific Party (1994) Russian-German Cooperation: The TRANSDRIFT I Expedition to the Laptev Sea, Ber. Polarforsch. 151, 168 pp.

Kassens, H., I. Dmitrenko, L. Timokhov and J. Thiede (1997) The TRANSDRIFT III Expedition: Freeze-up Studies in the Laptev Sea. In: Laptev Sea System: Expeditions in 1995, Kassens H. (ed.), Ber. Polarforsch. 248, 1-192.

Krylov, A.D. and A.G. Zatsepin (1992) Frazil ice formation due to difference in heat and salt exchange across a density interfase. J. Marine Systems, 3, 497-506.

Kuz,mina, N.P. (1980) About Oceanic Frontogenesis (in Russian). Izv. Akad.Nauk SSSR, Fizika atmosfery i okeana, 16, 10, 1082-1090.

Mac Vean, M.K. and J.D. Woods (1980) Redestribution of scalars during upper ocean frontogenesis. Quart. J. Roy. Met. Soc., 106, 448, 293-311.

Narimousa, S., R.R. Long and S.A. Kitaigorodskii (1986) Entrainment due to turbulent shear flow at the interface of a stably stratified fluid. Tellus, 38A, 1, 76-87.

Neshyba, S., V.T. Neal and W.W. Denner (1971) Temperature and conductivity measurements under Ice Island T-3. J. Geophys. Res., 76, 33, 8107-8119.

Oceanographic Tables (in Russian) (1975) Gidrometeoizdat, Leningrad, 476 pp.

Turner, J.S. (1965) The coupled turbulent transport of salt and heat across a sharp density interfase. Int. J. Heat and Mass Transfer, 8, 5, 759-767.

Turner, J.S. (1973) Bouyancy effects in fluids. Cambridge Univ. Press, 367 pp.

Woods, J.D. (1980) The generation of thermohaline finestructure at fronts in the ocean. Ocean modelling, 32, 1-4.

Zakharov, V.F. (1966) The Role of Trans-Fast Ice Polynyas in Hydrological Regime of the Laptev Sea (in Russian). Okeanologiya, Moscow, 6, 6, 1014-1022.

Zubov, N.N. (1963) Arctic Ice. U.S. Naval Oceanographic Office and Amer. Meteor. Soc., 491 pp.